Rare Metal Materials and Engineering
Volume 46, Issue 7, July 2017
Online English edition of the Chinese language journal

Cite this article as: Rare Metal Materials and Engineering, 2017, 46(7): 1756-1761.

ARTICLE

Electrodeposition of Iridium in 1-Butyl-3-Methylimidazolium Tetrafluoroborate Ionic Liquid

Qian Jiangang[1,2], **Li Xin**[1,2], **Luan Haijing**[1,2], **Li Tiejun**[1,2], **Yin Ying**[1,2]

[1] Key Laboratory of Bio-Inspired Smart Interfacial Science and Technology of Ministry of Education, [2] Beihang University, Beijing 100191, China

Abstract: The electrochemical behaviors of iridium electrodeposited in 1-butyl-3-methylimidazolium tetrafluoroborate ionic liquid were studied. Cyclic voltammograms prepared on the gold electrode suggested that Ir(III) was reduced to iridium with an irreversible one-step process, which was controlled by the diffusion of Ir(III). The diffusion rate is 3.83×10^{-11} m^2/s and the average transfer coefficient is 0.083. The morphology of iridium coatings prepared on molybdenum substrates was observed by scanning electron microscopy (SEM), and the composition was characterized by X-ray diffraction (XRD) and X-ray photoelectron spectroscopy (XPS). Results show that the morphologies of iridium coatings is dependent on the potential, the time and the current density of electrodeposition. Compact coatings are obtained at the reduction peak potential with a balance between the nucleation rate and the growth rate. Flat and compact coatings are formed when the current density ranges from 0.5 mA/cm^2 to 1.82 mA/cm^2 in the galvanostatic electrodeposition.

Key words: ionic liquid; iridium; potentiostatic electrodeposition; galvanostatic electrodeposition

Molybdenum has high specific strength, high melting point, low density and high thermomechanical loads. However, molybdenum is very easy to be oxidized when the temperature is higher than 600 ℃. It's necessary to prepare an oxidation resistant coating to protect molybdenum substrates when they are used in oxygen atmosphere at high temperature. Iridium with a melting point as high as 2400 ℃, good chemical and thermal inertness, strong resistance to oxygen and carbon at high temperature, is a promising candidate coating for oxidation-resistance and corrosion-resistance[1]. Moreover, iridium is the only metal which has high strength, high melting point and excellent oxidation resistance at the same time[2]. How to prepare iridium coatings with good properties has attracted extensive attention in recent years. According to early reports, iridium coatings were prepared mainly by the sputtering physical vapor deposition [3], chemical vapor deposition [4,5], plasma spray, double glow plasma [6-8], electrodeposition [9-12] etc. The vapor deposition methods always have high capital investment owing to the use of delicate reactors and vacuum systems. Moreover, they are not viable for complex mass production. Iridium coatings formed by plasma spray cannot be used as protective coatings especially in high temperature environment because of high porosity. Double glow plasma will result in high residual stress in iridium coatings. By contrast, electrodeposition which involves low equipment cost, is easy to handle and feasible to complex electrodes. Electrodeposition in the molten salt at high temperature encounters some disadvantages such as the high energy consumption and the strong corrosion to substrates. The performance of iridium coatings electrodeposited in the aqueous solution is not satisfactory because of the cathodic side reactions.

The room-temperature ionic liquids (RTILs) are generally called as room-temperature molten salts, presenting many excellent physical and chemical properties, such as low melting point, good thermal stability and chemical stability, high conductivity, low vapor pressure and good solubility with many organics or inorganics[13-15]. Due to the wide thermal

---

Received date: July 14, 2016
Foundation item: National Natural Science Foundation of China (51071014); Aviation Sports Association of China (2010ZE51055)

Corresponding author: Qian Jiangang, Ph. D., Associate Professor, School of Chemistry and Environment, Beihang University, Beijing 100191, P. R. China, Tel: 0086-10-82339870, E-mail: qianjg@buaa.edu.cn

and electrochemical windows, RTILs are sometimes regarded as the link between aqueous/organic solutions and high-temperature molten salts, and they can be used as the electrolytes for the electrodeposition of some metals and semiconductors, such as Al, Ti, Ta, Nb, Mo, and W, which could not always be achieved in aqueous solutions [16-19]. Moreover, the low water content in RTILs can efficiently avoid the hydrogen evolution reaction, and thus deposits will have better mechanical properties. In the present study, we report the electrochemical behaviors of iridium electrodeposited on the gold electrode in 1-Butyl-3-methylimidazolium tetrafluoroborate ionic liquid ($BMIMBF_4$). Even granular and compact iridium coatings were prepared on molybdenum substrates in $BMIMBF_4$ by the potentiostatic and galvanostatic electro- deposition, respectively.

1 Experiment

The preparation of electrolyte solution and all electrochemical experiments were conducted in an argon-filled glove box. The electrodeposition electrolyte was prepared by admixing 1-Butyl-3-methylimidazolium tetrafluoroborate (Shanghai Chengjie, >99%) with anhydrous iridium chloride "$IrCl_3$" (Shanxi Kaida, >99.5%) under continuous stirring for 2 h until $IrCl_3$ was fully dissolved. Cyclic voltammogram measurements and potentiostatic experiments were carried out in a conventional three-electrode cell using a electrochemical workstation (Shanghai Chenhua, CHI660D) combined with a digital recorder. The gold electrode (diam.=2 mm) and molybdenum sheets (immersed area =15 mm×2 mm×2 mm) were used as working electrodes. Platinum wire (diam. =0.5 mm) and graphite rod (diam.=3 mm) were used as a quasi-reference electrode[20] and a counter electrode, respectively. Galvanostatic experiments were conducted in a two-electrode cell with a DC(direct current) regulated current power supply (Beijing Dahua, DH1719A-4). The molybdenum sheet and the graphite rod were used as the cathode and anode electrode, respectively.

Ionic liquids and $IrCl_3$ were dried under vacuum for 24 h to reduce the moisture content before deposition. Molybdenum substrates were treated successively by polishing with abrasive papers, immersing in 5 wt% NaOH solution for 5 min to remove surface grease and washing with ethanol (Beijing Chemical Works, >99.5%), followed by drying for deposition. After electrodeposition, the working electrode was taken out from the electrodeposition solution carefully, washed with ethanol and distilled water, and then stored in desiccator for microstructure investigations after drying. Scanning electron microscope (SEM, Quanta 250 FEG) was used to observe surface morphologies of iridium coatings. X-ray diffraction (XRD, Shimadzu 6000) and X-ray photoelectric spectroscopy (XPS, PHI5300) were used to determine their compositions.

2 Results and Discussion

2.1 Electrochemical behaviors of $IrCl_3$ in $BMIMBF_4$ ionic liquid

Fig.1 displays the cyclic voltammograms of the gold electrode in the pure $BMIMBF_4$ and the $BMIMBF_4$ solution containing 67 mmol/L $IrCl_3$ with a scan rate of 0.05 V/s. The electrochemical window of $BMIMBF_4$ ranged from 1.5 V to −2.4 V (vs Pt) at 25 ℃, up to 3.9 V. When the temperature was raised to 120 ℃, the electrochemical window reduced to 3.1 V. This reveals that the electrochemical window of the pure $BMIMBF_4$ will become narrow with the temperature rising. When $IrCl_3$ was added to $BMIMBF_4$, a single cathodic current peak at −0.9 V was observed, indicating that Ir(III) was reduced to Ir through one step reaction. The equation is:

$$Ir^{3+} + 3e^{-} \longrightarrow Ir \qquad (1)$$

Cyclic voltammograms of the $BMIMBF_4$ solution containing 67 mmol $IrCl_3$ at different scan rates are shown in Fig.2. One cathodic current peak was observed from −0.9 V to −1.0 V at cyclic voltammograms with different scan rates as well as an anodic current peak at about −0.5 V. The cathodic peak current (I_{pc})was different to the anodic peak current (I_{pa}), and the cathodic peak potential (E_p) moved to the negative side as the scan rate increased. These results indicate that the reduction process of Ir(III) in $BMIMBF_4$ is irreversible.

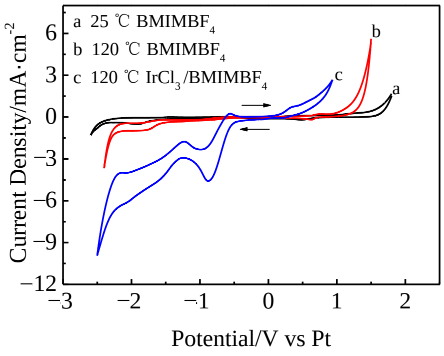

Fig.1 Cyclic voltammograms of the pure $BMIMBF_4$ and the $BMIMBF_4$ solution containing 67 mmol/L $IrCl_3$

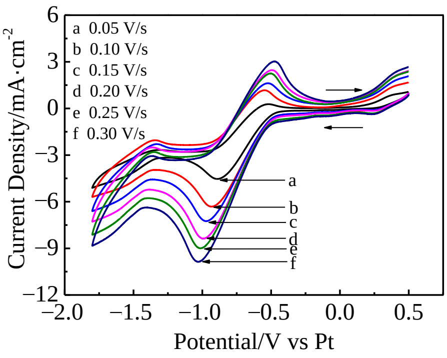

Fig.2 Cyclic voltammograms of the $BMIMBF_4$ solution containing 67 mmol/L $IrCl_3$ at scan rate ranging from 0.05 to 0.30 V/s at 120 ℃

There are following equations for irreversible electrode reaction[21]:

$$|E_p - E_{p/2}| = 1.857RT/(\alpha nF) \quad (2)$$

$$I_{pc} = 0.4958nFAC_oD^{1/2}v^{1/2}(\alpha nF/RT)^{1/2} \quad (3)$$

where, E_p and $E_{p/2}$ are the cathodic peak potential and the half cathodic peak potential (V), respectively; α is the transfer coefficient; n is the electron transfer number; F is Faraday constant (C/mol); I_{pc} is the cathodic peak current (A); A is the surface area of the working electrode (cm^2); C_o is the concentration of Ir(III) (mol/cm^3); D is the diffusion coefficient of Ir(III) in the ionic liquid; and v is the scan rate (V/s). The transfer coefficient of $IrCl_3$/$BMIMBF_4$ can be calculated according to Eq.(2), and the results are listed in Table 1. Thus, the average transfer coefficient was calculated as 0.083 in the $BMIMBF_4$ solution containing 67 mmol/L $IrCl_3$.

Fig.3a shows the relationship between the cathodic peak potential and the natural logarithm of scan rate (E_p vs ln$v$). The distinct linear relationship of E_p vs ln$v$ further demonstrates that the electrode reaction is irreversible. Fig. 3b shows the variations of cathodic peak currents vs the square root of scan rates. The cathodic peak current I_p increased with the square root of the scan rate in a linear relationship, which indicates that the electrode reaction is controlled by the diffusion process of Ir(III)[22]. The diffusion coefficient D in $BMIMBF_4$ solution containing 67 mM $IrCl_3$ was calculated to be 3.83×10^{-11} m^2/s from Fig.3b and Eq.(3).

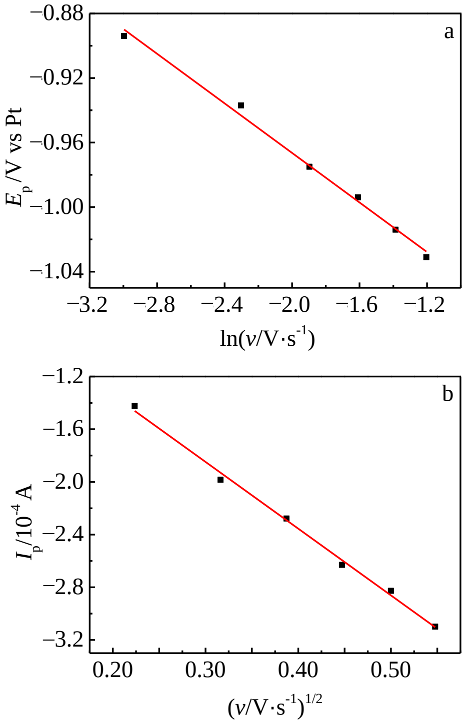

Fig. 3 Relationships between the cathodic peak potentials (E_p) (a) and the cathodic peak currents (I_p) (b) vs scan rates deduced from cyclic voltammograms in the $BMIMBF_4$ solution containing 67 mmol/L $IrCl_3$ at 120 ℃

2.2 Potentiostatic electrodeposition

The potentiostatic electrodeposition was carried out on the molybdenum substrate in the $BMIMBF_4$ solution containing 100 mmol/L $IrCl_3$ at 120 ℃. Fig. 4 displays the microstructures of iridium coatings prepared at different potentials for 12 h. The iridium coating formed at underpotential of −0.7 V is uneven and loose with many distinct protuberances and cracks on its surface. The coating obtained at the cathodic peak potential of −0.9 V is compact with few cracks, and consisted of many globular particles with size about from 200 nm to 500 nm. The iridium coating deposited at overpotential of −1.2 V was very loose like a bread, and there were many striking cracks on it. The particles are small (ca. 100 nm) and not exactly globular. Fukui and his co-workers[23] had studied the influence of potential on electrodeposition of silver in some ionic liquid, and they found that the deposition potential had a significant influence on the nucleation rate as well as the crystal growth mode. As the deposition potential changed in the negative direction, the nucleation was accelerated and the crystal growth mode was converted from isotropic to anisotropic. In this study, the nucleation rate was relatively slow ascribed to the small driving force at the underpotential of −0.7 V. The nucleation process occurred initially at the defects of the substrate, and then the particles grew up over these areas. These resulted in a nonuniform deposition process, so the deposit had many distinct protuberances, as shown in Fig.4a. With nucleation accelerated, the nucleation rate and the crystal growth rate reached a balance near the cathodic peak potential of −0.9 V. Fig.4b shows particles are globular with similar size, and the deposit is compact without clear cracks. At the overpotential of −1.2 V, the nucleation rate was further promoted. Because of the independence between the diffusion of Ir(III) and the potential, which limited the growth of iridium particles, particle size of iridium was small and the bonding force between particles was weak. As a result, deposits were loose with large cracks (Fig.4c).

Table 1 Data of cyclic voltammogram under different potential scan rates

v/V s^{-1}	I_p/ 10^{-4}A	E_p/V	$\|E_p - E_{p/2}\|$/V	α
0.05	−1.424	−0.890	0.219	0.096
0.10	−1.980	−0.942	0.247	0.085
0.15	−2.278	−0.976	0.257	0.082
0.20	−2.630	−0.992	0.260	0.080
0.25	−2.827	−1.014	0.266	0.079
0.30	−3.099	−1.031	0.274	0.077

Fig.5 shows the microstructures of iridium coatings deposited in the $BMIMBF_4$ solution containing 100 mmol/L $IrCl_3$ at 120 ℃ for different time. The potentiostatic electrodeposition was carried out at the cathodic peak potential of −0.9 V. More and more iridium particles were deposited as time increased, and

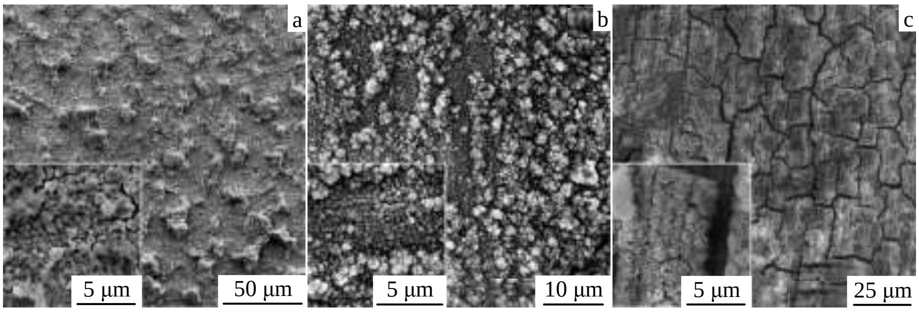

Fig.4 SEM images of Ir deposits prepared on the molybdenum substrate from the $BMIMBF_4$ ionic liquid containing 100 mmol/L $IrCl_3$ at 120 ℃ under different deposition potentials: (a) –0.70 V, (b) –0.90 V, and (c) –1.2 V

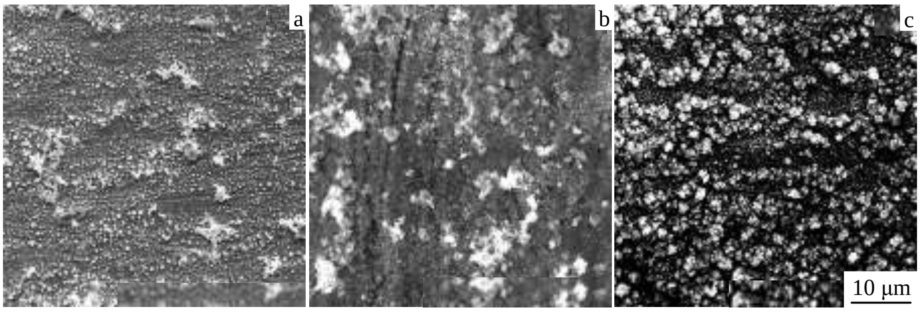

Fig. 5 SEM images of iridium coatings prepared in a $BMIMBF_4$ solution containing 100 mmol/L $IrCl_3$ at 120 ℃ for different deposition time: (a) 1 h, (b) 5 h, and (c) 12 h

eventually a coating consisted of iridium particles was formed. When deposited for 1 h, some particles with small size were scattered over the substrate. An integrated iridium coating was obtained when it deposited for 5 h. As the time increased, the iridium coating became compact but more rough, and particles were larger. This is probably owing to the fact that a balance between the nucleation rate and the crystal growth rate is more difficult to obtain around the whole substrate as deposition time increases.

2.3 Galvanostatic electrodeposition

In order to obtain a more smooth and compact iridium coatings, the galvanostatic electrodeposition was adopted. Fig. 6 shows the microstructure of iridium coatings prepared in the $BMIMBF_4$ ionic liquid containing 100 mM $IrCl_3$ at 120 ℃ by the galvanostatic electrodeposition with different current densities. One iridium coating with good properties will be difficult to obtain when the current density is too large or too small. And only when the current density ranged from 0.50 mA/cm^2 to 1.82 mA/cm^2, the quality of iridium coatings was relatively good. When the current density was 0.17 mA/cm^2, only few tiny iridium particles were deposited, without one integrated coating formed as displayed in Fig. 6a. This is probably because the weak nucleation and growth driving force leads to a slow deposition rate. When the current density rose to 0.50 mA/cm^2, the deposit was very smooth and defects on the surface were fewest. As the current density increased gradually, the iridium coating became more compact, but surface defects increased and the surface uniformity and flatness was destroyed. When the current density reached to 1.25 mA/cm^2, the iridium coating was most compact, but flatness and uniformity was not so good as that at 0.50 mA/cm^2. After that, the compactness of iridium coatings decreased as the current density increased further. When the current density reached 2.50 mA/cm^2, the iridium coating was neither uniform nor compact; furthermore, particles of the deposit were very small. Probably owing to the fact that the large current density leads to the quick nucleation rate, no enough cations are applicable to particles growth because of the restriction of the diffusion rate of Ir(III).

2.4 Composition analysis of the deposits

XPS spectra and XRD patterns of deposits are shown in Fig.7. The deposits were prepared in $BMIMBF_4$ solution containing 100 mmol/L $IrCl_3$ at 120 ℃ by the potentiostatic electrodeposition. The potential was −0.9 V and the deposition time was 12 h. Fig. 7a shows the result of XPS-peak- differentation-imitating analysis. From Fig.7a, we can see that two strong peaks appeared at 60.8 and 63.8 eV in the XPS spectrum of the deposit. It was confirmed that the deposits consisted of metallic iridium[1]. The weak peaks at 65.5 and 61.9 eV may represent the remaining $IrCl_3$ or its complex because of the incomplete cleaning. Three obvious 2θ peaks were found at 47.34°, 69.36° and 84.50° in Fig.7b, corresponding to the

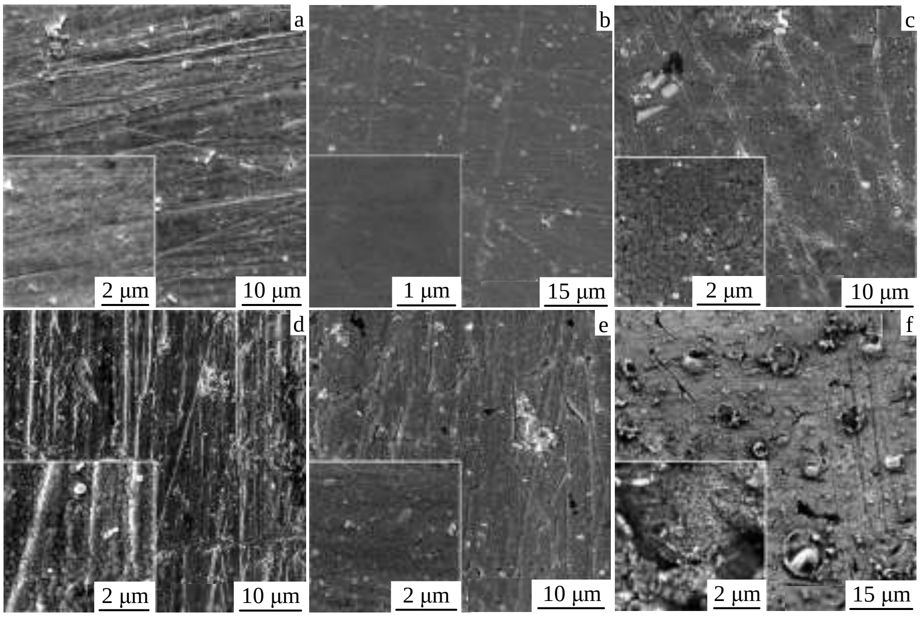

Fig. 6 Microstructures of the deposits on molybdenum substrates by the galvanostatic electrodeposition in the $BMIMBF_4$ solution containing 100 mmol/L $IrCl_3$ with different current densities at 120 ℃ for 12 h: (a) 0.17 mA/cm^2, (b) 0.50 mA/cm^2, (c) 0.67 mA/cm^2, (d) 1.25 mA/cm^2, (e) 1.82 mA/cm^2, and (f) 2.50 mA/cm^2

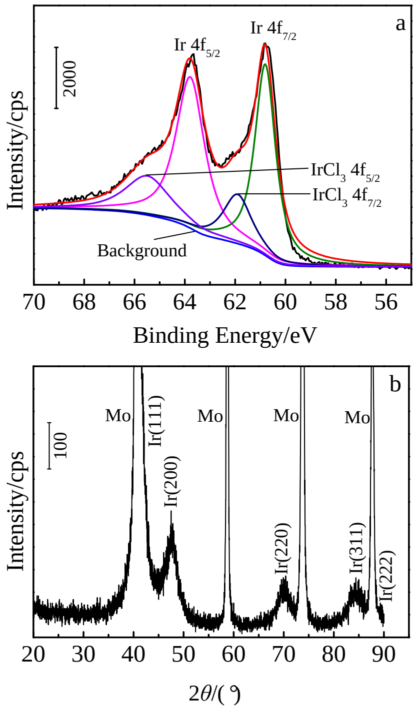

Fig. 7 XPS spectra (a) and XRD pattern (b) of the iridium coating electrodeposited on the molybdenum substrate from the $BMIMBF_4$ solution containing 100 mmol/L $IrCl_3$ at 120 ℃ under −0.9 V

(200), (220), (311) peaks of iridium according to the standard d-values taken from JCPDS (43-0144). Meanwhile, the (111) and (222) peaks at 40.68° and 88.00° were covered by the stronger peaks of the Mo substrate. The XRD pattern illustrated that the iridium coating had a polycrystalline structure[24].

3 Conclusions

1) Pure iridium coatings are obtained on the molybdenum substrate by the potentiostatic and the galvanostatic electrodeposition from the ionic liquid $BMIMBF_4$ at 120 ℃ in the argon atmosphere, and the coatings consist of metallic iridium with a polycrystalline structure.

2) From the cyclic voltammograms of iridium deposited on the gold electrode in the $BMIMBF_4$ solution at 120 ℃, we know that the reduction of Ir(III) to iridium takes place at −0.9 V vs Pt, which is an irreversible one-step process and controlled by the diffusion of Ir(III). The diffusion rate and transfer coefficient are 3.83×10^{-11} m^2/s and 0.083, respectively.

3) The potential and time in the potentiostatic electrodeposition have an important influence on the deposit morphologies. A compact iridium coating could be deposited at the cathodic potential peak. The coating tends to be loose and cracked when formed at the overpotential, and the coating will be rough and nonuniform at the underpotential. As the deposition time increases, the coating will be more compact but more rough meanwhile.

4) Iridium coatings with better quality could be obtained in the galvanostatic electrodeposition. The coating quality is dependent on the current density applied in deposition. Considering the compactness, flatness, uniformity and other factors, the best deposition condition is 0.50 mA/cm^2 at 120 ℃ in the $BMIMBF_4$ solution.

References

1 Le Vot S, Roué L, Bélanger D. *Electrochimica Acta*[J], 2012, 59: 49

2 Muñoz A G, Lewerenz H J. *Journal of The Electrochemical Society*[J], 2009, 156(5): D184

3 Mumtaz K, Echigoya J, Enoki H *et al*. *Journal of Materials Science*[J], 1995, 30(2): 465

4 Yan X, Zhang Q Y, Fan X D. *Materials Letters*[J], 2007, 61(1): 216

5 Bryskin B, Kostylev A, Pokrovsky J. *JOM*[J], 2012, 64(6): 682

6 Sekigawa T, Takeda F, Taguchital M. *The 8th Symposium on High Performance Materials for Severe Environments*[C]. Tokyo, 1997: 307

7 Wang L B, Chen Z F, Zhang P *et al*. *Journal of Coatings Technology and Research*[J], 2009, 6(4): 517

8 Wu W P, Chen Z F, Liu Y. *Plasma Science and Technology*[J], 2012, 14(10): 909

9 Etenko A, McKechnie T, Shchetkovskiy A *et al*. *ECS Transactions*[J], 2007, 3(14): 151

10 Zhu L A, Bai S X, Zhang H. *Surface and Coatings Technology*[J], 2011, 206(6): 1351

11 Qian J G, Xiao S M, Zhao T *et al*. *Rare Metal Materials and Engineering*[J], 2012, 41(7): 1139

12 Qian J G, Zhao T. *Transactions of Nonferrous Metals Society of China*[J], 2012, 22(11): 2855

13 Bonhote P, Dias A P, Papageorgiou N *et al*. *Inorganic Chemistry*[J], 1996, 35(5): 1168

14 Rogers R D, Seddon K R. *Science*[J], 2003, 302(5646): 792

15 Ohno H. *Electrochemical Aspects of Ionic Liquids, 2nd ed*[M]. Hoboken, N J: John Wiley & Sons Inc , 2005: 8

16 Endres F, MacFarlane D, Abbott A. *Electrodeposition from Ionic Liquids*[M]. Weinheim: Wiley-VCH Verlag GmbH & Co KGaA, 2008: 1

17 Armand M, Endres F, MacFarlane D R *et al*. *Nature Materials*[J], 2009, 8(8): 621

18 Simka W, Puszczyk D, Nawrat G. *Electrochimica Acta*[J], 2009, 54(23): 5307

19 Yang Z, Yuan R J, Liang Z H. *Rare Metal Materials and Engineering*[J], 2014, 43(3): 743 (in Chinese)

20 Bomparola R, Caporali S, Lavacchi A *et al*. *Surface & Coatings Technology*[J], 2007, 201(24): 9485

21 Bard A J, Faulkner L R. *Electrochemical Methods: Fundamentals and Applications, 2nd ed*[M]. New York: John Wiley & Sons, 2001: 157

22 Gunawardena G, Hills G, Montenegro I *et al*. *Journal of Electroanalytical Chemistry and Interfacial Electrochemistry*[J], 1982, 138(2): 225

23 Fukui R, Katayama Y, Miura T. *Journal of the Electrochemical Society*[J], 2011, 158(9): D567

24 Wang L B, Chen Z F, Zhang Y *et al*. *International Journal of Refractory Metals and Hard Materials*[J], 2009, 27(3): 590

1-丁基−3-甲基咪唑四氟硼酸盐离子液体电沉积制备 Ir 研究

钱建刚[1,2]，李鑫[1,2]，栾海静[1,2]，李铁军[1,2]，殷英[1,2]

(1. 仿生智能界面科学与技术教育部重点实验室，北京 100191)

(2. 北京航空航天大学，北京 100191)

摘　要：研究了在离子液体 1-丁基-3-甲基咪唑四氟硼酸盐中电沉积制备 Ir 的电化学行为，在金电极上获得的循环伏安特性曲线显示，Ir(III)经过一步还原反应生成 Ir，并且该反应是由 Ir(III)离子的扩散控制的不可逆过程。其中，扩散速率为 3.83×10^{-11} m^2/s，平均传质系数为 0.083。用扫描电镜(SEM)、X-射线衍射(XRD)及 X-射线光电子能谱(XPS)研究了在钼基体上获得的 Ir 层的表面形貌及组成，结果表明，Ir 层的形貌与沉积电位、时间及电流密度有关。恒电位电沉积过程中，在还原峰电位处由于成核及生长速率达到平衡，可以获得相对致密的镀层。在恒电流电沉积中，当电流密度在 0.5~1.82 mA/cm^{2}时，可以得到平整致密的 Ir 镀层。

关键词：离子液体；铱；恒电位电沉积；恒电流电沉积

作者简介：钱建刚，男，1964 年生，博士，副教授，北京航空航天大学化学与环境学院，北京 100191，电话：010-82339870，E-mail: qianjg@buaa.edu.cn